Bulletin of the *Transilvania* University of Braşov • Vol. 17 (66) No. 2 – 2024
Series I: Engineering Sciences
https://doi.org/10.31926/but.ens.2024.17.66.2.2

MODAL AND INERTIAL DECOMPOSITION OF WIND-INDUCED ENERGY STATE

F. BLAGA[1] P. ALEXA[1]

Abstract: *This paper presents a numerical approach for investigating the energy state of a planar steel shear frame subjected to turbulent wind loads. The objective is to illustrate the modal and inertial distribution of induced and dissipated energy generated by time varying wind forces. Time histories of wind pressure were acquired for a time period of 600 s from a bluff body Computational Fluid Dynamic turbulence model. Structural response, induced by highly arbitrary wind loads, is expressed by modal participation functions numerically assessed via Duhamel convolution integral. Modal decomposition functions are further derived and integrated into induced and dissipated energy components.*

Key words: *CFD, Duhamel, modal, wind loading, energy.*

1. Introduction

Wind induced forces on Civil Engineering structures are largely applied as equivalent static loads [16] assuming the "quasi-steady" theory [9]. Quasi-steady assumption is the basis of many wind loading code provisions [4] where wind-induced pressure is assumed to follow wind velocity variations upstream the analysed structure and wind speed fluctuations around a measured mean is treated by "gust loading factor", originally proposed by [5].

Air flow over rough surfaces such as urban areas leads to variation of the wind velocity both in time and space. Turbulent wind is currently simulated by experimental approach in wind tunnels or numerically predicted through Computational Fluid Dynamics (CFD). Several mathematical turbulence models [13] are integrated in finite element analysis software that allows for fluid flow simulation.

The main scope of the paper is to highlight the variation in time and space of wind velocity and pressure with the use of CFD [2] and to transfer the generated wind dynamic forces to a planar flexible structure.

Dynamic analysis of structures subjected to spatiotemporally varying wind forces [14] opens the door for an energy approach in structural assessment [10]. The time-history analysis performed in this paper focus on the modal distribution of induced and dissipated energy. The energy approach highlights new aspects of structural behaviour expanding

[1] Faculty of Civil Engineering, Technical University of Cluj-Napoca, Romania.

the range of dynamic modal analysis.

Wind stochastic nature [12] leads to highly arbitrary dynamic loading. Structural dynamic response is, in this paper, expressed by the widely known Duhamel's Integral or Convolution Integral. Simpson's Rule is applied to numerical integrate over a definite time interval.

2. Wind Flow Simulation

2.1. CFD Model

In order to simulate turbulent wind flow a bounded computational domain, Figure 1, was modelled. Turbulent wind flow is generated by several bluff bodies [7] positioned in the air stream.

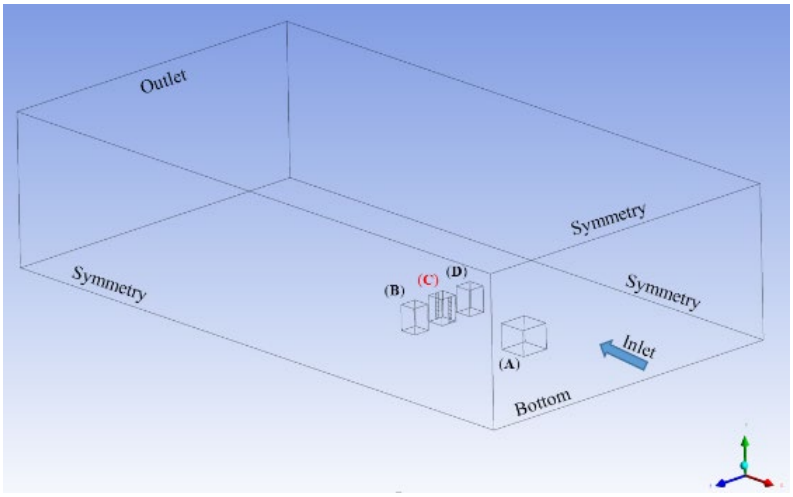

Fig. 1. *Computational domain*

The inlet plane of the solution domain is assigned as 35 m/s air velocity way in, the bottom is assigned as a Category III rough surface [4], the upper and the lateral parts are defined as symmetry boundary conditions. 3D dimensions of the computational domain, Figure 2, are based on provisions available in the literature [15].

Passive bluff-bodies A, B, and D were modelled in order to generate turbulent pressure on studied bluff-body C. Studied structure C have the spatial dimensions of an eleven storey structure, 43.60 m height and 30.0 m x 30.0 m ground surface. The solution domain mesh structure, Figure 3, consists of hexahedral elements [8]. Finer grid was generated close to the interest zone and a smooth transition from smaller to larger element sizes was achieved.

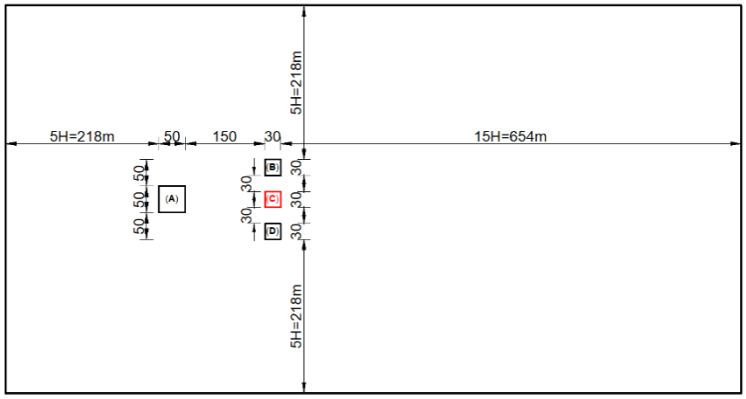

Fig. 2. *Computational domain, plan view*

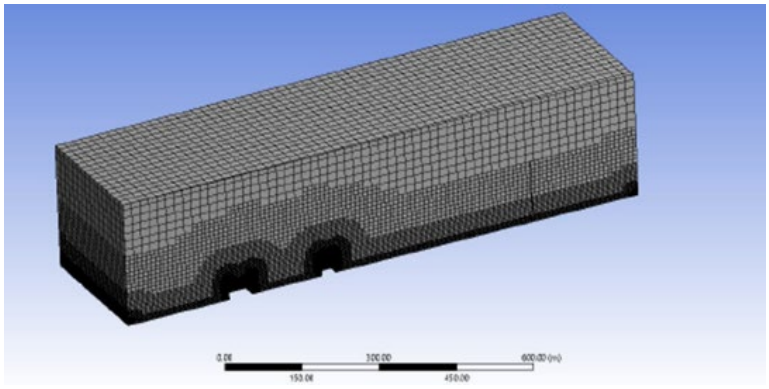

Fig. 3. *Mesh structure*

2.2. CFD Analysis Results

The simulated atmospheric boundary layer lead to turbulent flow around the square shaped structures. The instantaneous planar wind velocity distribution around the modelled bluff-bodies is illustrated in Figure 4. The turbulent flow is also highlighted by wind velocity variation over time. In Figure 5, simulated wind velocity in the upstream of the studied structure C is plotted over a 10 minutes interval at a time step of 1.0 s. Along-wind loads are related to the upstream and downstream faces of the studied structure. Simulated pressures are plotted in Figure 6 at 29.2 m height. On the upstream face of the studied structure C the load varies from pressure to suction while the downstream face is entirely subjected to suction. Wind speed dynamicity both in time and space leads to variable pressure on upstream and downstream faces and on the height of the structure.

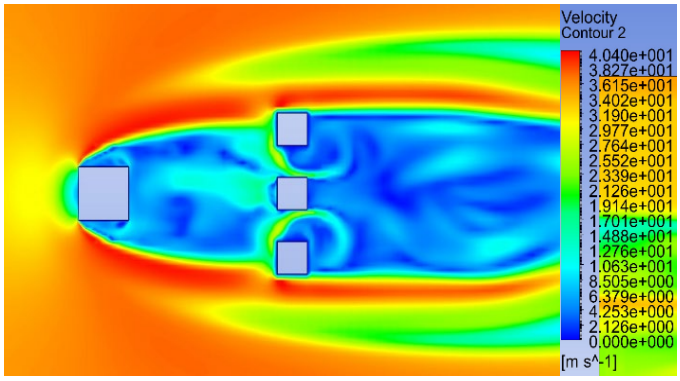

Fig. 4. *Velocity contour*

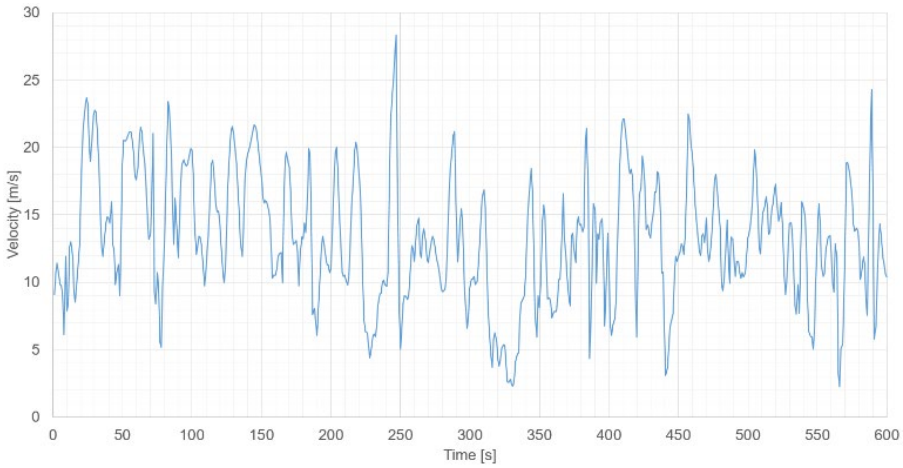

Fig. 5. *Wind velocity at 25.60 m height*

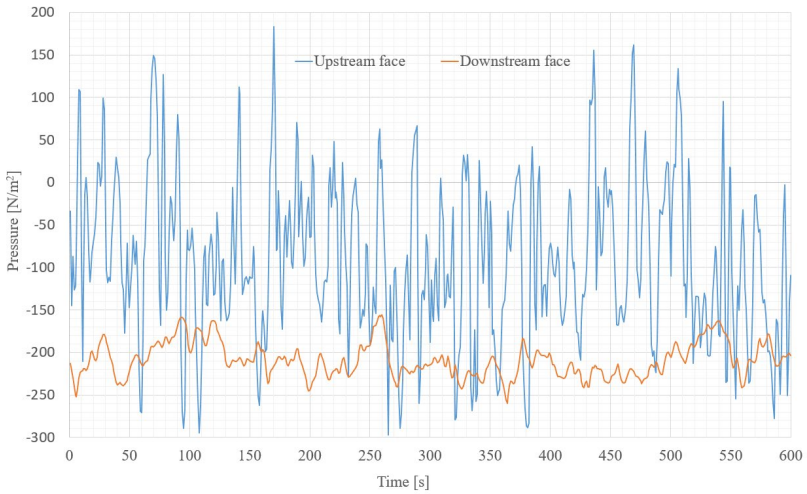

Fig. 6. *Wind pressure at 29.20 m height*

3. Modal Distribution of Energy Response

The simulated pressure in the CFD analysis [1] is transferred in a structural dynamics problem. An eleven storey planar steel frame is discretized as a dynamic system with 12 degrees of freedom, lateral floor displacements, loaded with dynamic forces derived from simulated time-varying pressure. The objectives of the study is to analyse the share of the induced and dissipated wind energies from the inertial and modal points of view.

3.1. Methodology

A numerical procedure is developed to analyse the dynamic response of a shear steel frame. Twelve degrees of freedom, lateral floor displacements x_1, x_2,..., x_m,..., x_{12}, are considered as depicted in Figure 7. The mass of the structure is lumped at the floor levels m_1, m_2,..., m_m,..., m_{12}. The applied forces $P_1(t)$, $P_2(t)$,..., $P_m(t)$,..., $P_{12}(t)$ are computed from CFD analysis as the sum of upstream and downstream pressure concentrated on a 6.0 m x 3.6 m surface, Figure 8.

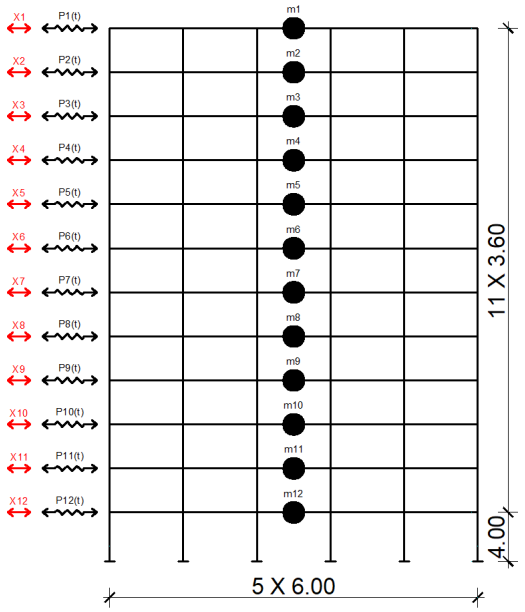

Fig. 7. *Dynamic 12 DOF system*

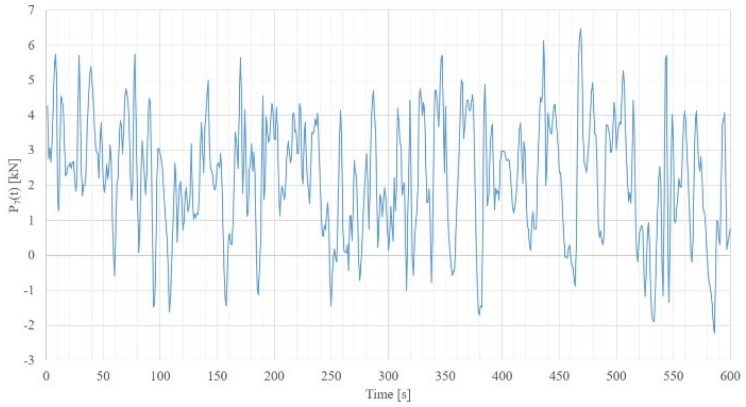

Fig. 8. *Applied forces $P_7(t)$*

3.2. Modal Analysis

Free vibrations of linear multi degree of freedom (MDF) systems are governed by [3]

$$\boldsymbol{M} \cdot \ddot{\boldsymbol{x}}(t) + \boldsymbol{K} \cdot \boldsymbol{x}(t) = 0 \tag{1}$$

where $\boldsymbol{M}$ is the lumped mass matrix

$$\boldsymbol{M} = \begin{pmatrix} m_1 & \cdots & 0 \\ \vdots & \ddots & \vdots \\ 0 & \cdots & m_{12} \end{pmatrix}$$

and $\boldsymbol{K}$ is the stiffness matrix

$$\boldsymbol{K} = \begin{pmatrix} k_{1_1} & \cdots & k_{1_{12}} \\ \vdots & \ddots & \vdots \\ k_{12_1} & \cdots & k_{12_{12}} \end{pmatrix}$$

Displacements $\boldsymbol{x}(t)$ time variation function is described by the harmonic function

$$\boldsymbol{x}(t) = A \cdot \sin(\omega_n t + \varphi) \cdot \boldsymbol{\phi}_n \tag{2}$$

which leads to the matrix eigenvalue problem

$$[\boldsymbol{K} - \omega_n^2 \cdot \boldsymbol{M}] \cdot \boldsymbol{\phi}_n = \boldsymbol{0} \tag{3}$$

Natural circular frequencies ω_n and corresponding natural mode shapes of vibration $\boldsymbol{\phi}_n$ are determined by solving the eigenvalue and eigenvectors problem.

$$\boldsymbol{\phi}_n = \begin{pmatrix} \phi_{1,n} \\ \vdots \\ \phi_{m,n} \\ \vdots \\ \phi_{12,n} \end{pmatrix}$$

Period of vibration T_n, cyclic frequencies f_n and normalised mode shapes are presented in Figure 9 for the first three natural modes of vibration.

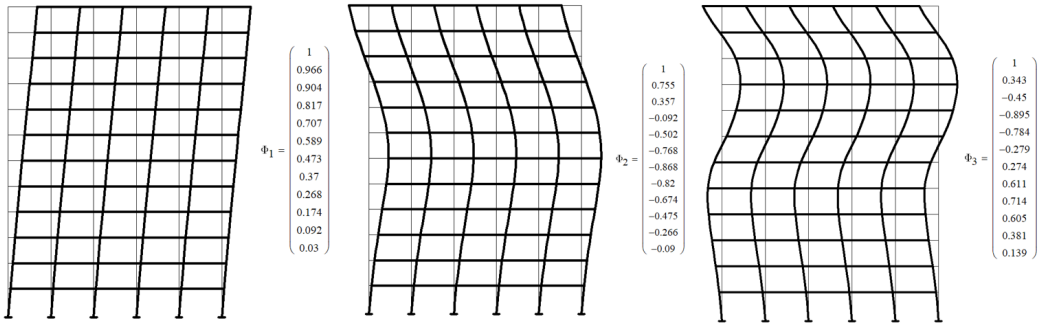

Fig. 9. *Natural mode shapes*

3.3. Response to Arbitrary Wind Forces

Dynamic behaviour of the studied structure is governed by the equation of motion [11]

$$\boldsymbol{M} \cdot \ddot{\boldsymbol{x}}(t) + \boldsymbol{C} \cdot \dot{\boldsymbol{x}}(t) + \boldsymbol{K} \cdot \boldsymbol{x}(t) = \boldsymbol{P}(t) \tag{4}$$

where $\boldsymbol{C}$ is the Caughey mass and stiffness proportional damping matrix [3]

$$\boldsymbol{C} = \boldsymbol{M} \cdot \sum_{l=0}^{J-1} a_l \cdot (\boldsymbol{M^{-1}} \cdot \boldsymbol{K})^l \tag{5}$$

$$\upsilon_n = \frac{1}{2} \cdot \sum_{l=0}^{J-1} a_l \cdot {\omega_n}^{2l-1} \tag{6}$$

for $J = 12$ modes with damping ration $\upsilon_n = 0.05$ for all modes. $\boldsymbol{P}(t)$ collects the applied forces

$$\boldsymbol{P}(t) = \begin{pmatrix} P_1(t) \\ \vdots \\ P_m(t) \\ \vdots \\ P_{12}(t) \end{pmatrix}$$

and the displacements $\boldsymbol{x}(t)$, velocities $\dot{\boldsymbol{x}}(t)$ and accelerations $\ddot{\boldsymbol{x}}(t)$ vectors describe the total dynamic response. Modal and inertial decomposition of nodal displacements, velocities and accelerations is expressed by the following linear transformations

$$x_{m,n}(t) = \phi_{m,n} \cdot \eta_n(t) \tag{7}$$

$$\dot{x}_{m,n}(t) = \phi_{m,n} \cdot \dot{\eta}_n(t) \tag{8}$$

$$\ddot{x}_{m,n}(t) = \phi_{m,n} \cdot \ddot{\eta}_n(t) \tag{9}$$

where m denotes floor / mass position and n denotes vibration mode. Modal, time dependent, coordinates $\eta_n(t)$ are evaluated via Duhamel convolution integral

$$\eta_n(t) = \frac{1}{M_n^* \cdot \omega_n^*} \cdot \int_0^t P_n^*(\tau) \cdot e^{-\upsilon_n \cdot \omega_n (t-\tau)} \cdot \sin \omega_n^* (t-\tau) d\tau \tag{10}$$

where

$$M_n^* = \boldsymbol{\phi}_n^T \cdot \boldsymbol{M} \cdot \boldsymbol{\phi_n} \tag{11}$$

$$P_n^*(\tau) = \boldsymbol{\phi}_n^T \cdot \boldsymbol{P}(\tau) \tag{12}$$

are the modal mass and force corresponding to n-th vibration mode and

$$\omega_n^* = \omega_n \cdot \sqrt{1 - \upsilon_n^2} \tag{13}$$

with damping ration $\upsilon_n = 0.05$ for all modes.

3.4. Energy Approach

Modal response in energy components requires the dynamic equilibrium equation to be expressed in modal coordinates

$$M_n^* \cdot \ddot{\eta}_n(t) + C_n^* \cdot \dot{\eta}_n(t) + K_n^* \cdot \eta_n(t) = P_n^*(t) \tag{14}$$

where

$$C_n^* = \boldsymbol{\phi}_n^T \cdot \boldsymbol{C} \cdot \boldsymbol{\phi_n} \tag{15}$$

$$K_n^* = \boldsymbol{\phi}_n^T \cdot \boldsymbol{K} \cdot \boldsymbol{\phi_n} \tag{16}$$

$$P_n^*(t) = \boldsymbol{\phi}_n^T \cdot \boldsymbol{P}(t) \tag{17}$$

are the modal damping, stiffness and force corresponding to n-th vibration mode.

Multiplying equation (14) by $d\eta_n(t) = \dot{\eta}_n(t)dt$ leads to

$$M_n^* \cdot \dot{\eta}_n(t) \cdot \ddot{\eta}_n(t) + C_n^* \cdot \dot{\eta}_n(t) \cdot \dot{\eta}_n(t) + K_n^* \cdot \eta_n(t) \cdot \dot{\eta}_n(t) = P_n^*(t) \cdot \dot{\eta}_n(t) \tag{18}$$

Integration of equation (18) leads to energy balance equation

$$\begin{aligned} &\int_0^t M_n^* \cdot \dot{\eta}_n(t) \cdot \ddot{\eta}_n(t) \cdot dt + \int_0^t C_n^* \cdot \dot{\eta}_n(t) \cdot \dot{\eta}_n(t) \cdot dt + \\ &+ \int_0^t K_n^* \cdot \eta_n(t) \cdot \dot{\eta}_n(t) \cdot dt = \int_0^t P_n^*(t) \cdot \dot{\eta}_n(t) \cdot dt \end{aligned} \tag{19}$$

in generalised modal coordinates η_n with $E_{\eta_n}^K$-kinetic energy, $E_{\eta_n}^D$-dissipated energy, $E_{\eta_n}^S$-strain energy, $E_{\eta_n}^I$-input energy.

$$E_{\eta_n}^K + E_{\eta_n}^D + E_{\eta_n}^S = E_{\eta_n}^I \tag{20}$$

Input and dissipated energy components are computed in this paper having the forms:

$$E_{\eta_n}^I = \int_0^t P_n^*(\tau) \cdot \dot{\eta}_n(\tau) \cdot d\tau \tag{21}$$

$$E_{\eta_n}^D = \int_0^t C_n^* \cdot \dot{\eta}_n(\tau) \cdot \dot{\eta}_n(\tau) \cdot d\tau \tag{22}$$

The above two energy components are, further, computed by numerical differentiation of $\eta_n(t)$ [17] and integrated via Simpson rule [6].

Inertial energy distribution is determined by the following linear transformations for every n mode shape,

$$E_{m,n}^I = \phi_{m,n} \cdot E_{\eta_n}^I \tag{23}$$

$$E_{m,n}^D = \phi_{m,n} \cdot E_{\eta_n}^D \tag{24}$$

and modal decomposition of input and dissipated energy for the entire structure is defined as follows.

$$E_n^I = \sum_{i=1}^{m} \left| E_{m,n}^I \right| \tag{25}$$

$$E_n^D = \sum_{i=1}^{m} \left| E_{m,n}^D \right| \tag{26}$$

Total energy response is acquired by linear combination of modal E_n^I and E_n^D components.

$$E^I = \sum_{i=1}^{n} E_n^I \tag{27}$$

$$E^D = \sum_{i=1}^{n} E_n^D \tag{28}$$

4. Numerical Results

Based on above theoretical development, further, the numerical results of the inertial and modal distributions of both, induced and dissipated energies are presented.

First, the total values of the two energy are presented graphically in Figure 10. It may be seen that a small value (cca. 7 kNm) of the total induced energy (cca. 50.00 kNm) is dissipated via natural damping level of 5% of critical damping ratio.

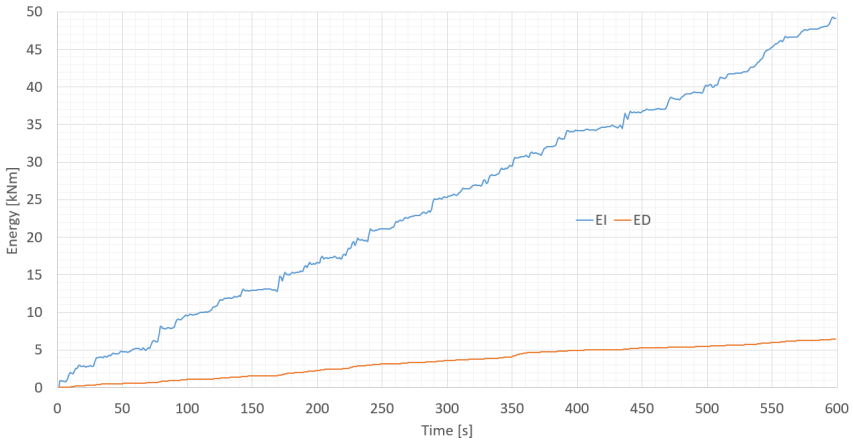

Fig. 10. *Total energy balance*

4.1. Modal distribution

Consistent with the objective of analysing modal distribution of the two energy components, the energy amounts associated to natural fundamental vibration mode are presented in Figure 11 against the total energy values.

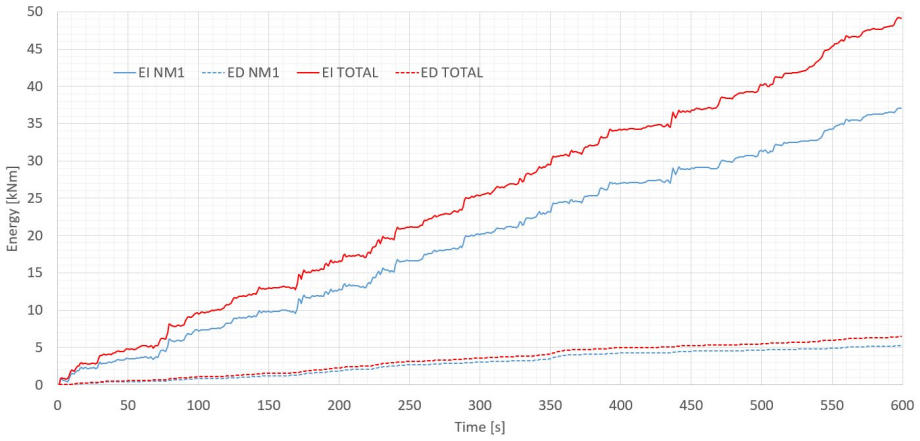

Fig. 10. *Total vs normal mode 1 energy balance*

Numerically, an amount of cca. 37.00 kNm of a total amount (cca. 50.00 kNm) is induced by the natural fundamental mode of vibration. In percentage terms, it represents 74%, while the remaining 26% is induced via the upper natural modes. These results of energy modal distribution are consistent with the modal distribution of dynamic response in lateral displacements. A detailed picture of modal distribution of both, induced and dissipated energies in the first three natural modes of vibration are presented in Figure 11. Again, the lion share of fundamental natural mode is emphasized.

4.2. Inertial distribution

Associated inertial state of planar vibratory motion induced by wind action is expressed by the lumped floor masses (Figure 7). Based on theoretical development expressed via equations 23, 24, the following graphically presented results emphasize inertial distributions of the two energy components: induced energy in Figure 11 and dissipated energy in Figure 12.

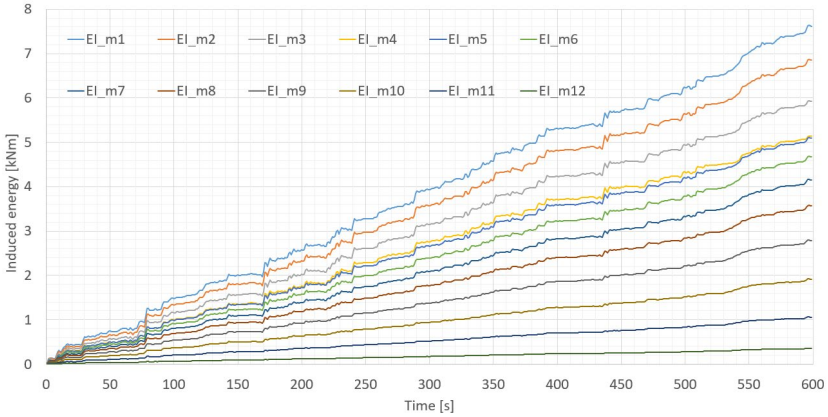

Fig. 11. *Inertial distribution of induced energy*

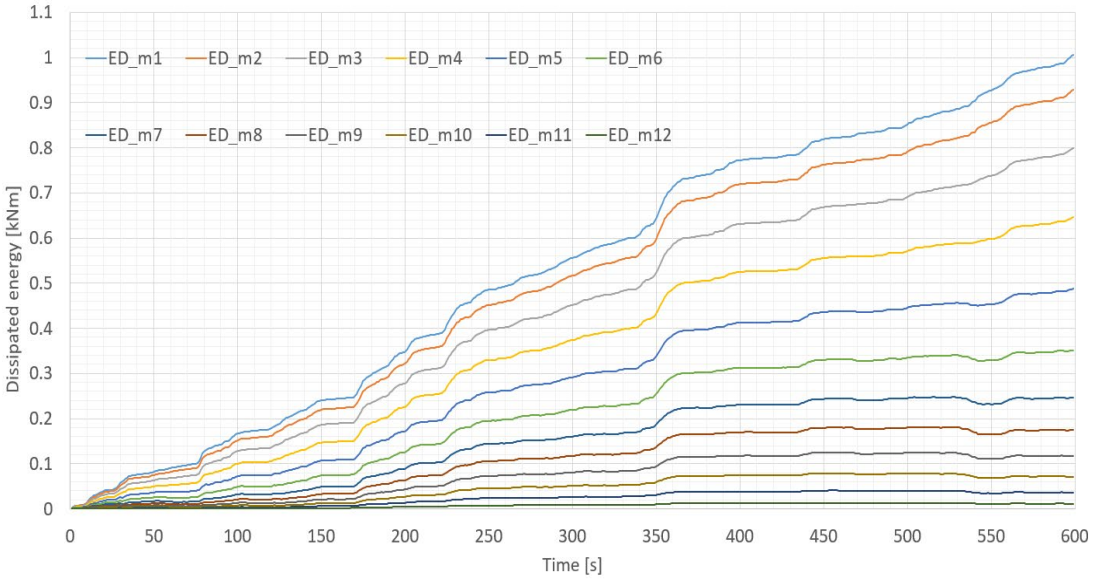

Fig. 12. *Inertial distribution of dissipated energy*

It must be mentioned that the lumped masses along the height of the structure are, practically equal. Therefore, the differentiating parameter in inertial distribution is expected to be, mainly, the velocities of masses. Indeed, as it can be seen in Figure 11 and Figure 12 the largest amounts of both, induced and dissipated energies are associated with upper masses that vibrate with the highest velocities.

Referring to induced energy, mass m_1 takes no less than 15% of the total induced amount. The same ratio of the dissipated energy via mass m_1 may be concluded. Emphasizing the share of the first three mases, a total of 22.5 kNm (45%) of induced energy is generated at the top three levels of the structure while, the dissipated ratio of the same masses is 42 % of the total dissipated energy.

5. Conclusions

The contribution fulfils two main objectives associated to dynamic response of multi-storey steel structures to dynamic wind action: an energy formulation of the dynamic response in terms of induced energy and dissipated energy via intrinsic linear viscous damping and the inertial and modal distributions of the energy state.

Traditional mechanical state of structural dynamic response is made up of the two classical components: static (sectional and unit stresses) and kinematic (displacements and deformations). Adding energy state to these components of the dynamic response, an augmented mechanical state is obtained. The authors of the present contribution are aware of the fact that the static and kinematic states are so popular that from students up to highly qualified engineers, everybody knows the associated numerical values of these parameters. It is, indeed, difficult to *translate* such a well-established fact into

energy terms. Nevertheless, the energy state enjoys a few advantages in expressing the dynamic response of a structure: it is a scalar quantity and, most important, it's synthetic nature includes the general and sectional geometry, the elastic state, the inertial state, the damping state and the dynamic actions all expressed via stiffness, mass, damping and forces matrices. Adding the energy state of the dynamic response to the traditional mechanical state is the main contribution of the present work.

References

1. Ansys, I. C. E. M. CFD : *ICEM CFD theory guide*. Ansys inc (2012).
2. Blocken, B.: *50 years of computational wind engineering: past, present and future*. In: Journal of Wind Engineering and Industrial Aerodynamics (129), 2014, pp. 69-102.
3. Chopra, A. K.: *Dynamics of structures. Theory and Applications to Earthquake Engineering*. New Jersey: Prentice Hall, 2007.
4. CR 1-1-4: *Wind action on structures, Romanian Standard*. ASRO, 2012.
5. Davenport, A. G.: *Gust loading factors*. In: Journal of the Structural Division, 93 (3), 1967, pp. 11-34.
6. Davis, P. J., Philip R.: Methods of numerical integration. New York. Dover Publications, 2007.
7. Elkhoury, M.: *Assessment of turbulence models for the simulation of turbulent flows past bluff bodies*. In: Journal of Wind Engineering and Industrial Aerodynamics (154), 2016, pp. 10-20.
8. Franke, J., et al.: *Recommendations on the use of CFD in predicting pedestrian wind environment*. In: Cost action C, 14, 2004.
9. Holmes, J. D.: *Wind loading of structures*. New York. Taylor & Francis 2015.
10. Iancovici, M., et al: *Nonlinear dynamic response analysis of buildings for wind loads. A new frontier in the structural wind engineering*. In: Journal of Building Engineering (47), 2022: 103708.
11. Ifrim, M.: *Structural Dynamics and Earthquake Engineering* (in Romanian). Bucharest. EDP, 1984.
12. Iversen, E. B., Juan, M. M., Jan K. M., Henrik, M.: *Short-term probabilistic forecasting of wind speed using stochastic differential equations*. In: International Journal of Forecasting, 32 (3), 2016, pp. 981-990.
13. Murakami, S.: *Overview of turbulence models applied in CWE*. In: Journal of Wind Engineering and Industrial Aerodynamics (74), 1997, pp. 1-24.
14. Rosa, L., Gisella, T., Alberto, Z., and Aly, A. M.: *Wind-induced dynamics and loads in a prismatic slender building: A modal approach based on unsteady pressure measurements*. In: Journal of Wind Engineering and Industrial Aerodynamics (107), 2012, pp. 118-130.
15. Tominaga, Y., et al.: *AIJ guidelines for practical applications of CFD to pedestrian wind environment around buildings*. In: Journal of wind engineering and industrial aerodynamics, 96 (10-11), 2008, pp. 1749-1761.
16. Zhou, Y., Kijewski, T., Kareem, A.: *Along-wind load effects on tall buildings: comparative study of major international codes and standards*. In: Journal of

Structural Engineering, 128 (6), 2002, pp. 788-796.
17. https://www.mathworks.com/matlabcentral/fileexchange/97267-numerical-differentiation-toolbox. Accessed: 06.07.2025.